Mendeleev Communications

Mendeleev Commun., 2026, **36**, 72–75

New metal-free dye with an acceptor-anchor group of thieno[3,2-*b*]thiophene family for dye-sensitized solar cells

Roman A. Irgashev,*[a] Alexander S. Steparuk,[a] Viktor V. Emets,[b] Ekaterina V. Tekshina,[c] Nikita M. Tolkach,[d] Petr I. Lazarenko,[d] Gennady L. Rusinov[a] and Sergey A. Kozyukhin[c]

[a] *I. Ya. Postovsky Institute of Organic Synthesis, Ural Branch of the Russian Academy of Sciences, 620137 Ekaterinburg, Russian Federation. E-mail: irgashev_ra@mail.ru, irgashev@ios.uran.ru*
[b] *A. N. Frumkin Institute of Physical Chemistry and Electrochemistry, Russian Academy of Sciences, 119071 Moscow, Russian Federation*
[c] *N. S. Kurnakov Institute of General and Inorganic Chemistry, Russian Academy of Sciences, 119991 Moscow, Russian Federation*
[d] *National Research University of Electronic Technology, 124498 Zelenograd, Moscow, Russian Federation*

DOI: 10.71267/mencom.7849

5-Methylene-6-oxo-5,6-dihydrothieno[3,2-*b*]thiophene-2-carboxylic acid was proposed as an electron-accepting unit in the design of organic donor–π–acceptor dye molecules. New organic dye incorporating a thieno[3,2-*b*]indole donor, a thiophene π-linker, and the abovementioned acceptor moiety was synthesized and evaluated as a photosensitizer for dye-sensitized solar cells. The photovoltaic device based on this dye achieved a power conversion efficiency of 0.95% with a short-circuit current density of 2.81 mA cm^{-2}, an open-circuit voltage of 0.54 V, and a fill factor of 0.63 under standard AM 1.5 G solar irradiation (100 mW cm^{-2}).

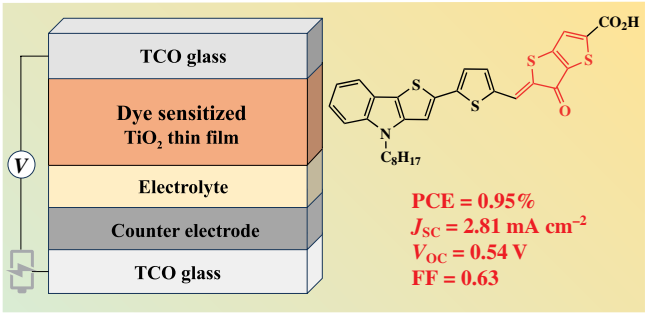

Keywords: thieno[3,2-*b*]thiophene, thieno[3,2-*b*]indole, D–π–A structure, metal-free organic dyes, dye-sensitized solar cells.

The innovative photovoltaic technology of dye-sensitized solar cells (DSSCs), reported for the first time by O'Regan and Grätzel in 1991,[1] has attracted great interest due to ready availability of the materials required for the construction of these devices, coupled with their lightweight nature.[2–5] In contrast to silicon-based solar cells, DSSCs can be fabricated using simpler, low-cost, and energy-efficient processes under ambient conditions. The ease of processing, coupled with the tunability of organic materials, has also spurred interest in other solar technologies, such as perovskite solar cells[6,7] and organic solar cells,[8] which similarly benefit from solution-processability, material versatility, and lower energy demands for their fabrication. In addition, DSSCs have high operational efficiency along with remarkable adaptability, allowing integration into a variety of environments and products.[9]

The main working elements of DSSC devices are a nanocrystalline metal oxide semiconductor layer, most commonly titanium dioxide (TiO_2), organic photosensitizer, an electrolyte, and a counter electrode.[10,11] Among them, organic dye is a key component significantly affecting both the power conversion efficiency and the longevity of solar devices. There are two main types of dyes for DSSCs, usually ruthenium-based organic complexes,[12] and more promising metal-free organic dyes.[13–15] Metal-free dye molecules typically have a donor–π-bridge–acceptor (D–π–A) architecture, which facilitates efficient charge separation, broad absorption spectrum in the visible and near-infrared range, resistance to the photo-degradation, controlled dye aggregation, minimized charge recombination, suitable HOMO and LUMO energy levels, robust intramolecular charge transfer, as well as an anchoring group in the acceptor part of dye molecule, which ensures reliable attachment to the metal oxide as a semiconductor surface.[16] For the design of metal-free dye structures, the following compounds are often used: electron-rich heteroaromatics, for instance, indole-fused heterocycles, for the donor fragment, thiophene units for the π-bridge, 2-cyanoacrylic acid for the acceptor-anchoring part.[17] Thieno[3,2-*b*]indole (TI) ring-system has found application as a donor part in the structure of dyes for DSSCs, as well as other photo- and electroactive materials, due to its planarity, extended π-conjugation, and easy routes to fine-tune the electronic and optical properties through chemical modification of its framework.[18] Indeed, the D–π–A TI-based dyes exhibited promising results in DSSCs, achieving power conversion efficiency (PCE) comparable to that of reference organic photosensitizers.[19–21] In this context, the elaboration of new D–π–A architectures with the TI scaffold to find efficient photosensitizer dyes is of great importance for achieving high-performance DSSC devices.

Previously, we synthesized three series of D–π–A dyes (Figure 1) containing TI ring-system as a donor part, thiophene unit as a π-bridge part, and 2-cyanoacrylic acid (**A**),[22,23] 5-(methylene)barbituric acid (**B**)[23] or 5-(methylene)rhodanine-3-acetic acid (**C**)[24] as an acceptor-anchoring part, and used these dyes as photosensitizers for DSSCs. The DSSCs using dyes **A** exhibited promising performance, achieving PCE in the range of 2.25–3.02% under standard AM 1.5 G illumination. In contrast, DSSCs based on dyes **B** demonstrated significantly lower efficiency, with PCE values ranging from 0.20 to 0.32% under

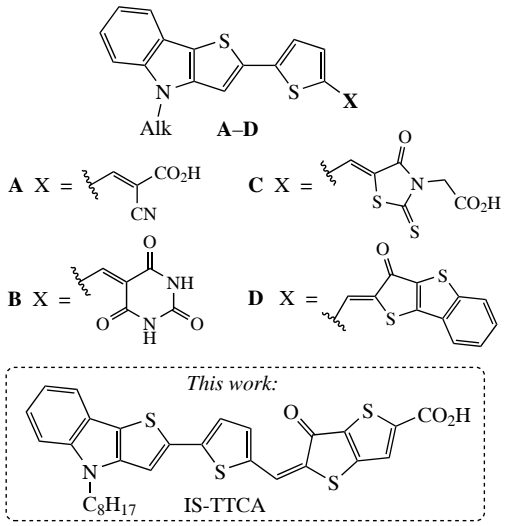

Figure 1 The structures of TI-based materials **A**–**D** used for photovoltaics and dye IS-TTCA.

the same conditions. In turn, solar cells sensitized with dyes **C** shown PCE values in the range of 0.42 to 1.09%.

In continuation of our metal-free dye study, we wish to report herein the synthesis and application as a photosensitizer for DSSCs of new dye IS-TTCA with D–π–A structure, comprising thieno[3,2-*b*]indole, thiophene, and 5-methylene-6-oxo-5,6-dihydrothieno[3,2-*b*]thiophene-2-carboxylic acid (TTCA) parts (see Figure 1). To design dye IS-TTCA structure, compound **D** was considered as a basis since it showed efficiency values up to 12.02% for transport materials in perovskite solar cells (PSCs).[25] To this end, benzene ring in benzo[*b*]thieno[2,3-*d*]thiophen-3(2*H*)-one part of structure **D** was removed to leave thieno-[3,2-*b*]thiophen-3(2*H*)-one followed by attachment of carboxy group at position 5 to provide the anchoring property of new TTCA acceptor part.

Dye IS-TTCA (Scheme 1) was obtained according to the same strategy as for dyes **A**–**D**, wherein 2-(thiophen-2-yl)-thieno[3,2-*b*]indole **1** was utilized as a TI-based substrate with the completed 'donor–π-bridge' structure suitable for the next construction of D–π–A molecules. Compound **1** was N-alkylated with 1-bromooctane followed by the Vilsmeier formylation to afford TI-linked thiophene-2-carbaldehyde **3**. Then, the Knoevenagel condensation of aldehyde **3** with 6-hydroxy-thieno[3,2-*b*]thiophene-2-carboxylic acid **4** results in the desired product **5** (IS-TTCA).

To evaluate the potential of the synthesized dye IS-TTCA as a photosensitizer for DSSCs, its photophysical and

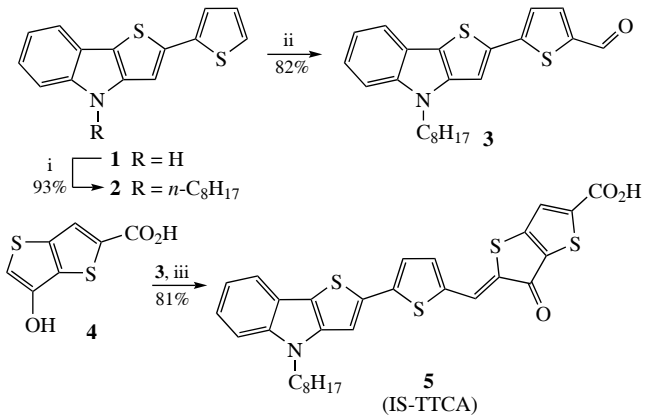

Scheme 1 *Reagents and conditions*: i, *n*-$C_8H_{17}Br$, NaH, DMF, 20 °C, 24 h; ii, $Me_2NC(O)H$, $POCl_3$, $CHCl_3$, 20 °C, 48 h; iii, pyrrolidine, AcOH, 120 °C, 1 h.

electrochemical properties were thoroughly investigated, followed by the assessment of its performance in a complete device. The isodensity surface plots of the electron-density distributions of the highest occupied molecular orbital (HOMO) and the lowest unoccupied molecular orbitals (LUMO) for IS-TTCA are shown in Figure S1 (see Online Supplementary Materials). The calculations showed that the HOMO of IS-TTCA was predominantly localized on the TI donor part and the thiophene π-linker, whereas the LUMO of this molecule was predominantly localized on the TTCA acceptor part and also the thiophene π-linker. This distribution of HOMO and LUMO levels in IS-TTCA molecules indicates that, upon light excitation, the transition from HOMO to LUMO can be regarded as a charge transfer transition, which ultimately promotes photoinduced electron transfer from the dye to the TiO_2 layer. The calculated HOMO and LUMO energy levels at –5.42 eV and –3.09 eV, respectively, yield a HOMO–LUMO gap of 2.33 eV, which is close to the optically found band gap ($E_{0\text{–}0}$ = 2.09 eV). This consistency supports the reliability of the electronic structure predictions.

The UV-VIS absorption spectrum of IS-TTCA in a THF solution [Figure 2(*a*)] exhibits two prominent absorption regions (Table 1). The maximum wavelength absorption at 300–425 nm can be assigned to the localized π–π* electronic transitions within the dye molecule. More importantly for DSSC applications, a broad absorption band is observed in the visible region (425–650 nm). This longer-wavelength absorption is attributed to an intramolecular charge transfer (ICT) from the electron-donating TI fragment to the electron-accepting TTCA moiety anchored to the semiconductor surface. The significant molar absorption coefficient (ε) of 38 700 $dm^3\ mol^{-1}\ cm^{-1}$ for this visible band indicates reasonable light-harvesting efficiency, which is a crucial factor for generating photocurrent in a DSSC.

Upon excitation, dye IS-TTCA exhibits emission at 655 nm. However, the photoluminescence quantum yield (Φ_{em}) and the excited-state lifetime (τ) were found to be relatively low, at 7% and 0.49 ns, respectively. This suggests that non-radiative decay pathways are highly competitive with radiative relaxation (emission). The calculated high non-radiative rate constant (see Table 1) confirms this. In a DSSC setup, efficient electron injection from the excited dye molecule into the TiO_2 conduction band is paramount. A short excited-state lifetime and substantial non-radiative decay imply that a significant portion of excited electrons relax back to the ground state within the dye molecule itself before they can be effectively injected into the semiconductor. This process is detrimental to

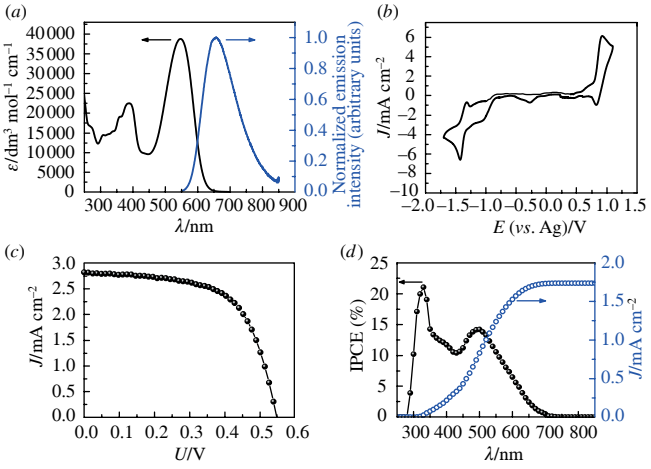

Figure 2 (*a*) The absorption and emission spectra in THF; (*b*) cyclic voltammograms; (*c*) *J*/*V* curves of DSSCs and (*d*) IPCE spectra of dye IS-TTCA.

Table 1 Optical data of the dye IS-TTCA.

λ_{max}[a]/nm	ε[a]/dm^3 mol^{-1} cm^{-1}	Photoluminescence							E_{0-0}[g]/eV
		λ_{ex}[a]/nm	λ_{em}[a]/nm	$\Delta\nu$[b]/cm^{-1}	Φ_F[c]	τ[d]/ns	$k_r \times 10^9$[e]/s^{-1}	$k_{nr} \times 10^9$[f]/s^{-1}	
547	38700	542	655	3183	0.07	0.49	0.14	1.90	2.09
389	22400								
309	14400								

[a]In THF. [b]Stokes shift. [c]Absolute quantum yield. [d]Lifetime of luminescence. [e]Radiative rate obtained from equation $k_r = \Phi_F/\tau$. [f]Non-radiative rate obtained from equation $k_{nr} = k_r(\Phi_F^{-1} - 1)$. [g]Band gap E_{0-0} was derived from the intersecting point of absorption and normalized emission spectra in THF.

the overall charge separation and consequently limits the photocurrent generation.[26]

Electrochemical characterization using cyclic voltammetry [see Figure 2(*b*)] was performed to determine the redox properties and estimate the frontier molecular orbital energy levels of IS-TTCA. The parameters of the study were as follows: $E_{ox}^{onset} = 0.78$ V; $E_{red}^{onset} = -1.35$ V; $E_{HOMO} = -5.44$ eV; $E_{HOMO} = -3.31$ eV; $\Delta E_{gap}^{el} = 2.13$ eV.† The calculated HOMO energy level of IS-TTCA is sufficiently lower than the redox potential of the I^-/I_3^- electrolyte (–4.8 eV). This energy alignment indicates that dye regeneration, where the oxidized dye molecule accepts an electron from the electrolyte, is thermodynamically favorable. Furthermore, the calculated LUMO energy level is appropriately positioned relative to the conduction band edge of TiO_2 (–3.9 eV). This favorable alignment suggests that electron injection from the excited dye into the TiO_2 conduction band is also thermodynamically permissible. Thus, based on the electrochemical properties, both the injection and regeneration steps, which are essential for sustained photocurrent generation, appear to be energetically feasible for IS-TTCA in a DSSC employing the standard iodide/triiodide electrolyte.

The photovoltaic performance of DSSC device sensitized with dye IS-TTCA was evaluated under simulated AM 1.5 illumination [see Figure 2(*c*)]. The cell exhibited a power conversion efficiency (PCE) of 0.95 ± 0.05%, with a short-circuit photocurrent density (J_{SC}) of 2.81 ± 0.03 mA cm^{-2}, an open-circuit photovoltage (V_{OC}) of 0.54 ± 0.01 V, and a fill factor (FF) of 0.63 ± 0.02. These average performance parameters, along with their standard deviation errors, were calculated by statistically processing the results obtained from three devices. The incident photon to current conversion efficiency (IPCE) spectrum [see Figure 2(*d*)] shows photocurrent generation across the absorption range of the dye, correlating well with the UV-VIS absorption profile. Noticeable peaks were observed around 330 nm (21%) and 500 nm (14%), corresponding to the π–π* and ICT absorption bands, respectively. The shape of the IPCE spectrum confirms that the dye is indeed acting as the sensitizer and light absorption leads to charge collection.

Comparing the different characterization results allows for an understanding of the device performance. While the electrochemical data indicate that the energy levels of IS-TTCA are suitable for injection and regeneration, and the absorption spectrum shows reasonable light harvesting potential with a decent molar extinction coefficient, the relatively low observed PCE and J_{SC} are likely limited by the excited-state kinetics of the dye. The short excited-state lifetime and high non-radiative decay rate, as revealed by the photoluminescence studies, strongly suggest that the rate of electron injection into TiO_2 is significantly hindered by competing de-excitation pathways within the dye itself. This results in a lower number of electrons successfully transferred to the semiconductor per absorbed photon, directly impacting the J_{SC}. Although the V_{OC} and FF are also contributing factors to the overall efficiency, the measured photophysical properties point to poor electron injection kinetics as a primary bottleneck for this sensitizer.

In summary, we have successfully synthesized dye IS-TTCA containing the donor part of the thieno[3,2-*b*]indole ring-system and the acceptor-anchor part of the TTCA fragment with the thieno[3,2-*b*]thiophene core, which is the first example of its application for DSSC dyes. While dye IS-TTCA possesses favorable energy levels for charge transfer and promising light absorption, its modest photovoltaic performance was primarily attributed to significant non-radiative decay processes limiting excited-state lifetime and electron injection efficiency. These results highlight a critical area for improvement in this new class of dyes, and future development of dye molecules should focus on suppressing non-radiative decay pathways.

This study was supported by The Russian Science Foundation (grant no. 24-23-00402).

The authors are grateful to G. A. Kim for carrying out DFT calculations that were performed using the 'Uran' supercomputer of the Institute of Mathematics and Mechanics of the Ural Branch of the Russian Academy of Sciences. The authors also express their gratitude to Dr. E. F. Zhilina for performing UV-VIS measurements.

Analytical studies were carried out using equipment of the Center for Joint Use 'Spectroscopy and Analysis of Organic Compounds' at the Postovsky Institute of Organic Synthesis of the Ural Branch of the Russian Academy of Sciences.

Online Supplementary Materials

Supplementary data associated with this article can be found in the online version at doi: 10.71267/mencom.7849.

References

1 B. O'Regan and M. Grätzel, *Nature*, 1991, **353**, 737; https://doi.org/10.1038/353737a0.
2 J. Gong, J. Liang and K. Sumathy, *Renewable Sustainable Energy Rev.*, 2012, **16**, 5848; https://doi.org/10.1016/j.rser.2012.04.044.
3 J. Gong, K. Sumathy, Q. Qiao and Z. Zhou, *Renewable Sustainable Energy Rev.*, 2017, **68**, 234; https://doi.org/10.1016/j.rser.2016.09.097.
4 C. Dragonetti and A. Colombo, *Molecules*, 2021, **26**, 2461; https://doi.org/10.3390/molecules26092461.
5 B. K. Korir, J. K. Kibet and S. M. Ngari, *Energy Sci. Eng.*, 2024, **12**, 3188; https://doi.org/10.1002/ese3.1815.
6 S. A. Kuklin, S. V. Safronov, A. S. Peregudov, E. A. Khakina, M. M. Babaskina, M. G. Ezernitskaya, O. Yu. Fedorovskii, E. S. Kobeleva, L. V. Kulik, L. A. Frolova, P. A. Troshin and A. R. Khokhlov, *Mendeleev Commun.*, 2024, **34**, 316; https://doi.org/10.1016/j.mencom.2024.04.003.
7 E. A. Komissarova, S. A. Kuklin, N. A. Slesarenko, A. F. Latypova, A. F. Akbulatov, V. V. Ozerova, M. N. Kevreva, N. A. Emelianov, L. A. Frolova and P. A. Troshin, *Mendeleev Commun.*, 2025, **35**, 327; https://doi.org/10.71267/mencom.7632.
8 E. A. Komissarova, S. A. Kuklin, P. M. Kuznetsov, A. N. Galiullin, N. A. Slesarenko and P. A. Troshin, *Mendeleev Commun.*, 2025, **35**, 413; https://doi.org/10.71267/mencom.7708.
9 A. Agasti, L. Peedikakkandy, R. Kumar, S. P. Mohanty, V. P. Gondane and P. Bhargava, in *Springer Handbook of Inorganic Photochemisry*, Springer, Cham, 2022, pp. 1137–1214; https://doi.org/10.1007/978-3-030-63713-2_39.

† $E_{HOMO} = -[E_{ox}^{onset} - E_{1/2}(Fc/Fc^+) + 4.8]$, where $E_{1/2}(Fc/Fc^+)$ is the half-wave potential of the Fc/Fc^+ couple against the Ag electrode (defined at 0.14 V in the calibration experiment). $E_{LUMO} = E_{0-0} + E_{HOMO}$.

10 A. Hagfeldt, G. Boschloo, L. Sun, L. Kloo and H. Pettersson, *Chem. Rev.*, 2010, **110**, 6595; https://doi.org/10.1021/cr900356p.
11 S. Rahman, A. Haleem, M. Siddiq, M. K. Hussain, S. Qamar, S. Hameed and M. Waris, *RSC Adv.*, 2023, **13**, 19508; https://doi.org/10.1039/D3RA00903C.
12 M. Grätzel, *J. Photochem. Photobiol., C*, 2003, **4**, 145; https://doi.org/10.1016/S1389-5567(03)00026-1.
13 S. Chaurasia and J. T. Lin, *Chem. Rec.*, 2016, **16**, 1311; https://doi.org/10.1002/tcr.201500288.
14 A. Sen, M. H. Putra, A. K. Biswas, A. K. Behera and A. Groβ, *Dyes Pigm.*, 2023, **213**, 111087; https://doi.org/10.1016/j.dyepig.2023.111087.
15 C.-P. Lee, R. Y.-Y. Lin, L.-Y. Lin, C.-T. Li, T.-C. Chu, S.-S. Sun, J.-T. Lin and K.-C. Ho, *RSC Adv.*, 2015, **5**, 23810; https://doi.org/10.1039/c4ra16493h.
16 X.-L. Wang, J.-F. Huang, J.-M. Liu and P. Tsiakaras, *Coord. Chem. Rev.*, 2025, **522**, 216143; https://doi.org/10.1016/j.ccr.2024.216143.
17 P. R. Nitha, S. Soman and J. John, *Mater. Adv.*, 2021, **2**, 6136; https://doi.org/10.1039/D1MA00499A.
18 S. Pandey, S. Aggarwal, R. Choudhary and S. K. Awasthi, *RSC Adv.*, 2022, **12**, 15787; https://doi.org/10.1039/D1RA09233B.
19 X.-H. Zhang, Y. Cui, R. Katoh, N. Koumura and K. Hara, *J. Phys. Chem. C*, 2010, **114**, 18283; https://doi.org/10.1021/jp105548u.
20 Y. K. Eom, S. H. Kang, I. T. Choi, Y. Yoo, J. Kim and H. K. Kim, *J. Mater. Chem. A*, 2017, **5**, 2297; https://doi.org/10.1039/c6ta09836c.
21 J.-M. Ji, H. Zhou, Y. K. Eom, C. H. Kim and H. K. Kim, *Adv. Energy Mater.*, 2020, **10**, 2000124; https://doi.org/10.1002/AENM.202000124.
22 A. S. Steparuk, R. A. Irgashev, G. L. Rusinov, E. V. Krivogina, P. I. Lazarenko and S. A. Kozyukhin, *Russ. Chem. Bull.*, 2019, **68**, 1208; https://doi.org/10.1007/s11172-019-2542-z.
23 A. S. Steparuk, R. A. Irgashev, E. F. Zhilina, V. V. Emets, V. A. Grinberg, E. V. Krivogina, E. V. Belova, P. I. Lazarenko, G. L. Rusinov and S. A. Kozyukhin, *J. Mater. Sci.: Mater. Electron.*, 2022, **33**, 6307; https://doi.org/10.1007/s10854-022-07805-w.
24 A. S. Steparuk, R. A. Irgashev, E. F. Zhilina, V. V. Emets, V. A. Grinberg, E. V. Tekshina, E. V. Belova, P. I. Lazarenko, N. M. Tolkach, G. L. Rusinov and S. A. Kozyukhin, *Mendeleev Commun.*, 2022, **32**, 523; https://doi.org/10.1016/j.mencom.2022.07.030.
25 A. S. Steparuk, R. A. Irgashev, E. F. Zhilina, G. L. Rusinov, S. A. Petrova, D. S. Saranin, A. E. Aleksandrov and A. R. Tameev, *New J. Chem.*, 2022, **46**, 16612; https://doi.org/10.1039/D2NJ02202H.
26 G. Boschloo, *Front. Chem.*, 2019, **7**, 77; https://doi.org/10.3389/fchem.2019.00077.

Received: 11th June 2025; Com. 25/7849